

# Development and Performance Investigation on a 60kW Induction Motor for EV Propulsion

Yon-Do Chun<sup>\*\*\*</sup>, Byoung-Gun Park<sup>\*\*\*</sup>, Dong-Jun Kim<sup>\*</sup>, Jae-Hak Choi<sup>\*</sup>, Pil-Wan Han<sup>†</sup> and Sukkee Um<sup>\*\*</sup>

**Abstract** – This paper introduces the development process and investigation of a 60kW induction motor for electric vehicles. We present performance improvement in the induction motor of electric vehicle using copper die-casting based on a multi-gate process. Copper die-casting motors can reduce the size of the motor, the loss of the rotor, and material costs. We also introduce electromagnetic, thermal, mechanical design and analysis results that satisfy the design and the performance requirements. In order to analyze losses accurately of induction motor, commercial finite element analysis is done considering PWM voltage and thermal characteristics by using lumped-circuit parameters. Experimental tests are also carried out to validate the traction motor design.

**Keywords:** High speed, Induction motor, EV, Traction motor, Copper die-casting rotor

## 1. Introduction

Due to the growing popularity of hybrid and electrical vehicles, traction electric motors are becoming common in the automotive industry [1-4]. The most common form of induction motor utilizes a squirrel-cage rotor, which is composed of a series of longitudinal conductor bars inserted into slots located towards the periphery of a stack of steel laminations. In this study, we designed a 60kW-12,000rpm induction motor for electric vehicles and demonstrate performance improvement of the induction motor using copper die-casting based on a multi-gate process [7, 8]. The multi-gate die-casting process enabled us to obtain a high quality casting product decreasing casting defects from fluid, such as gas traps and mixing of inclusion particles. In addition, copper die-casting motors can reduce the size of motors, the loss of the rotor, and material costs. We include electromagnetic, thermal, mechanical design and analysis that satisfy the design and performance requirements. The electromagnetic dimensions of the motor were determined from the induction motor equivalent circuit and verified from FEM analysis in various operating [5, 6]. In order to accurately analyze the losses of the induction motor, we made a commercial finite element analysis considering the thermal characteristics using a three-dimensional computational flow dynamic analysis. The mechanical designs were made considering structural safety and the vibration response and the thermal

conditions from the analysis results. We also made experimental tests on the continuous (30kW) and maximum (60kW) operating conditions to validate the performance of the traction motor design.

## 2. Design of EV Motor

### 2.1 Performance requirement of motor

The EV motor described in this paper was designed to satisfy the continuous (30kW) and maximum power (60kW) operating conditions as shown in Table 1 and Fig. 1. The motor was designed using an input voltage at the base speed (3,000rpm) and 60% (130V) of the rated voltage. It was increased to the rated voltage (220V) at the maximum speed (12,000rpm) to prevent a decrease in power in the high speed region.

### 2.2 Design parameters and specifications of the motor

Table 1 shows the design parameters and specifications of the EV induction motor designed for 3,000rpm (base operating speed) using a 130V/100Hz supply voltage; however, it can work up to 12,000rpm.

**Table 1.** Specification of EV motor

| Items   | Characteristic       | Unit   | Value                        |                     |
|---------|----------------------|--------|------------------------------|---------------------|
| Output  | Max. condition       | Power  | kW                           | 60@ 3,000~12,000rpm |
|         |                      | Torque | Nm                           | 190@ 0~3,000rpm     |
|         | Continuous condition | Power  | kW                           | 30@3000~12,000rpm   |
|         |                      | Torque | Nm                           | 95.5@0~3,000rpm     |
| Cooling | Cooling method       | -      | Water cooling (water jacket) |                     |
| Voltage | Line to Line         |        | V                            | 130Vrms @ 3,000rpm  |
|         |                      |        |                              | 220Vrms @ 12,000rpm |

† Corresponding Author: Electric Motor Research Center, Korea Electrotechnology Research Institute Korea. (pwhan@keri.re.kr)

\* Electric Motor Research Center, Korea Electrotechnology Research Institute Korea

\*\* School of Mechanical Engineering, Hanyang University, Korea.

\*\*\* Department of Energy and Power Conversion Engineering, Korea University of Science & Technology, Changwon, Korea.

Received: May 11, 2015; Accepted: November 29, 2015

**Table 2.** Design parameters

| Items                      | Unit                  | Value  |
|----------------------------|-----------------------|--------|
| Output coefficient         | $[10^3 \times J/m^3]$ | 212    |
| Aspect ratio( $L/\tau_p$ ) |                       | 1.27   |
| Out diameter of stator     | mm                    | 260    |
| Inner diameter of stator   | mm                    | 160    |
| Stack length               | mm                    | 160    |
| Current density of stator  | A/mm <sup>2</sup>     | 11.0   |
| Current density of rotor   | A/mm <sup>2</sup>     | 7.99   |
| Flux density of airgap     | T                     | 1.1    |
| Electrical steel thickness | mm                    | 0.35   |
| Core loss at 1.5T/100hz    | [W/kg]                | 55     |
| Rotor conductor            |                       | copper |

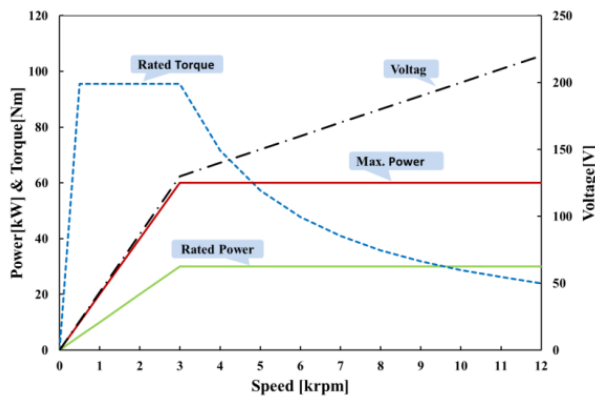


**Fig. 1.** Rated performance vs speed

### 3. Analysis Method of EV Motor

#### 3.1 Electromagnetic analysis

The basic losses, the copper loss and the iron loss, were calculated by 2D electro-magnetic FEM using sinusoidal voltage.

The induction motor was analyzed by time-varying magnetic finite element analysis at the rated conditions (130V/100Hz) using sinusoidal voltage. Fig. 3 shows the flux density distribution. The maximum value of the stator yoke and the teeth flux density were 1.45 [T] and 1.3 [T],

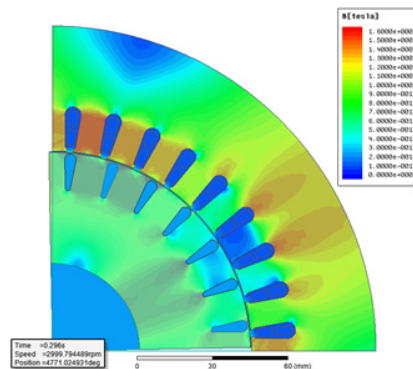


**Fig. 2.** Flux density distribution

**Table 3.** Comparison of the loss analysis and test results

| Method | Eff. [%] | Cur. [A] | Tor. [Nm] | Losses [W]    |              |      |       |            |
|--------|----------|----------|-----------|---------------|--------------|------|-------|------------|
|        |          |          |           | Stator copper | Rotor copper | Iron | Mech. | Stray load |
| FEM    | 92.2     | 173.0    | 92.0      | 950           | 430          | 350  | 68    | 750        |
| ECM    | 92.2     | 171.7    | 96.8      | 1073          | 438          | 217  | 68    | 750        |

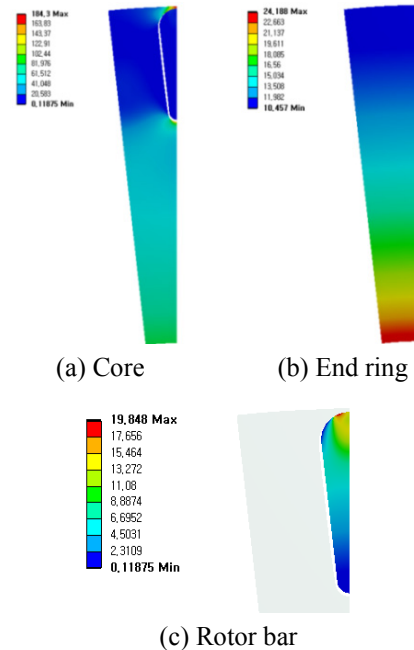


**Fig. 3.** Mechanical stress analysis

respectively.

Table 3 shows the loss analysis by a 2D FEM and equivalent circuit method of the induction motor. Because this machine is driven by a PWM inverter, the efficiency can decrease due to harmonic loss. The stator winding and rotor bar temperature were set at 100°C and 130°C, respectively. The stray load loss was calculated at about 2.5% of output power and the mechanical loss was calculated using Takeuchi's formula [11]. In IEC-60034-2-1, the stray load loss was about 1.7% of the output power (1.6% of the input power) at a 60kW rating. In this study, the stray load loss was considered to be higher than the IEC standard because the EV motor is driven by a PWM inverter.

#### 3.2 Mechanical stress analysis

To verify the structural safety of the rotor, a stress analysis was performed on the rotor using centrifugal force on the maximum speed as shown in Fig. 3. The maximum stress values of the core, endring and rotor bar were 184, 24, 20 [Mpa], respectively, with safety factors above 2 and the yield strength of core was 380 [Mpa] and that of copper was 55[Mpa]. In the end-ring, the stress of the inner part was higher than that of the outer part because the area

**Table 4.** Physical properties of materials for the rotor

| Item                        | Shaft (SM45C) | Rotor core | Bar & Endring |
|-----------------------------|---------------|------------|---------------|
|                             | Steel         | 35PN250    | Copper        |
| Density(kg/m <sup>3</sup> ) | 7,850         | 7600       | 8,900         |
| Elastic Modulus(GPa)        | 210           | 200        | 110           |
| Poisson' ratio              | 0.3           | 0.3        | 0.33          |
| Yield strength(MPa)         | 505           | 370~385    | 62~69         |

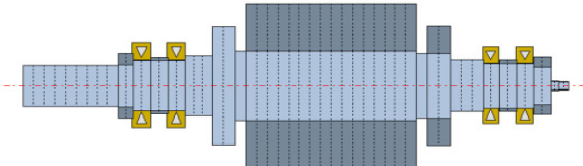
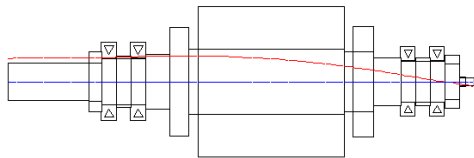
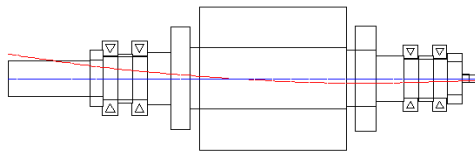


**Fig. 4.** Modelling of the rotor assembly



(a) 1<sup>st</sup> natural frequency (20,400 cpm)



(b) 2<sup>nd</sup> natural frequency (44,214 cpm)

**Fig. 5.** Modal analysis results

decreases toward the inner part with the same centrifugal force. This result shows that the rotor structure was structurally safe enough to withstand the centrifugal force at the maximum speed.

### 3.3 Modal analysis

A modal analysis of the rotor at maximum speed (12,000 [rpm]) was done to verify the rotor dynamics characteristics. Fig. 4 shows a modelling of the rotor assembly for FEM analysis, and Table 4 shows the physical properties of the components of the rotor assembly. Non-oriented electrical steel was used for the rotor core and the supported stiffness of the ball bearings was considered. As the 1<sup>st</sup> natural frequency was 20,400 [cpm] in the analysis results of Fig. 5, the safety factor was 70% compared with the maximum rotating speed, 12,000 [rpm]. The unit cpm is the abbreviation of cycles per minute, which indicates the natural frequency and critical speed in the rotating machine.

### 3.4 Thermal analysis

Three-dimensional computational flow dynamic analysis

**Table 5.** Comparison between the thermal test and the analysis

| Method   | Winding  | Stator   | Rotor     | Cage      |
|----------|----------|----------|-----------|-----------|
| Analysis | 110.3 °C | 100.6 °C | 128.66 °C | 128.67 °C |

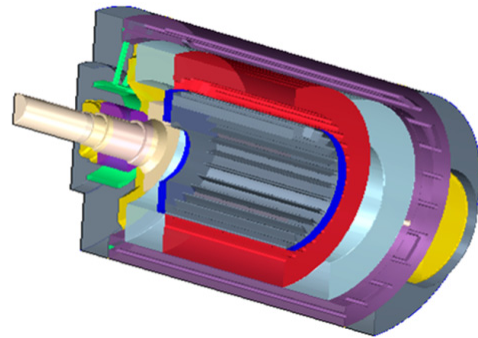


**Fig. 6.** 3D modelling for thermal analysis

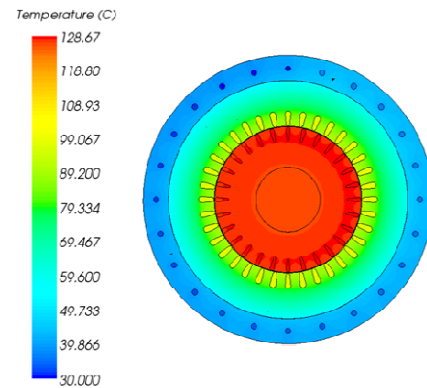


**Fig. 7.** Thermal analysis results

has been performed for the induction motor as shown in Fig. 6. Electromagnetic losses from the FEM analysis as in Table 3 were adopted as heat sources for the thermofluidic analysis.

Fig. 7 and Table 5 present the temperature distribution and maximum temperature in the specific components of the induction motor. The highest temperature in the motor was predicted to be approximately 129 °C in the rotor and cage with a negligible difference. There was a significant temperature difference between the rotor and stator because of the air gap. It should be also noted that the temperature of the winding part can be compared with thermal saturation test results.

## 4. Prototype and Test

Fig. 8 shows the process assembling prototype. The rotor bar was made by copper die-casting, and the stator was molded by a synthetic resin to improve cooling capacity.

Fig. 9 shows the test facility for the high speed machine presented in this paper. The test motor was driven by a

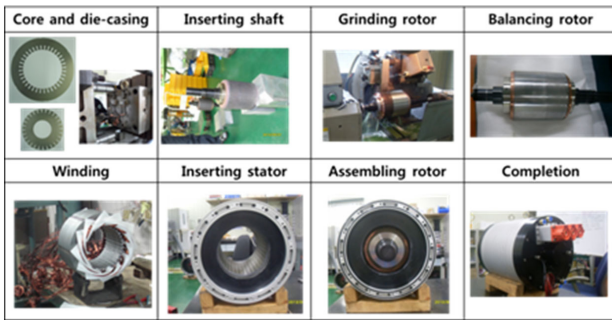


Fig. 8. Assembling prototype

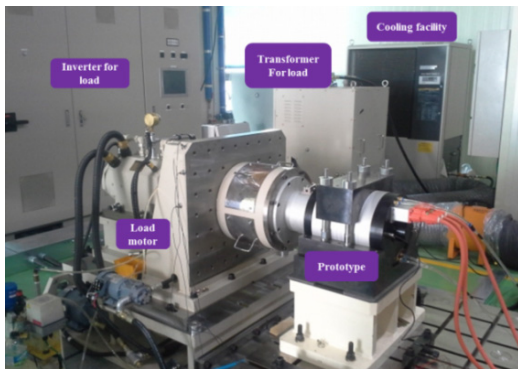


Fig. 9. Dynamo system for testing

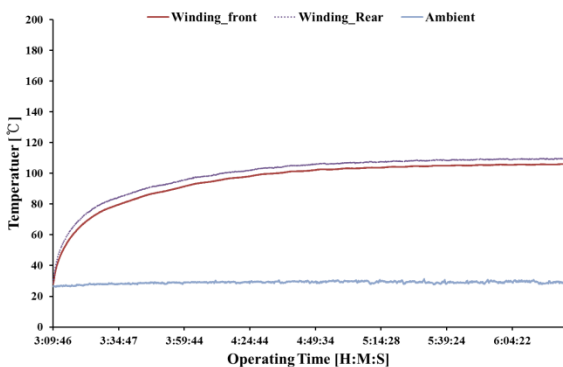


Fig. 10. Thermal saturation test (30kW\_30,000rpm)

commercial inverter and cooled by a water jacket. Fig. 10 shows the thermal saturation test on the base operating conditions (30kW at 3,000rpm) which can be compared with the thermal analysis results. The winding temperature was 109°C, which confirms the thermal analysis result (winding temperature: 110.3°C).

Figs. 11 and 12 respectively show the efficiency test results at 30kW and 60kW output power. One was done at temperature saturated conditions to consider continuous operating conditions, and the other was tested instantaneously for the maximum operating condition.

Fig. 13 shows the vibration test results according to the operating conditions. As the vibration characteristics are good under 2.8 [mm/s], the limit of ISO 10816-3, the modal analysis is verified.

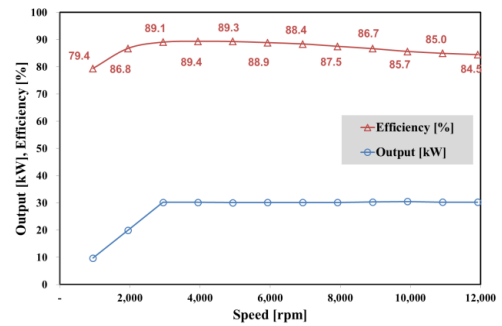


Fig. 11. Efficiency and output test (30kW)

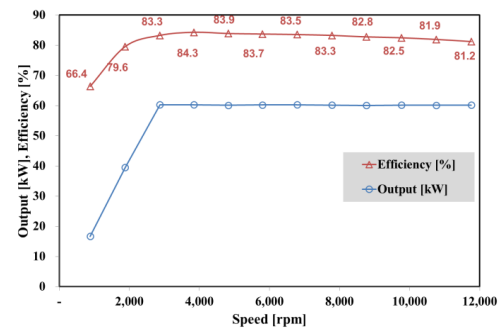


Fig. 12. Efficiency and output test (60kW)

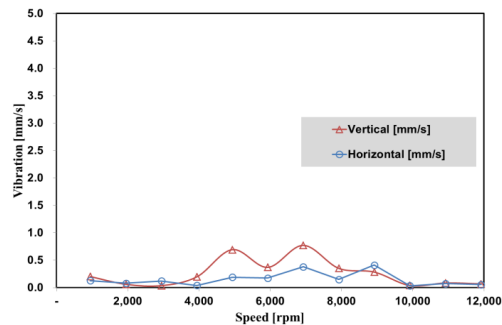


Fig. 13. Vibration test

## 5. Conclusion

Recently, the induction motor has drawn more interest for electrical traction because it is less expensive, robust, and inherently safe in case of inverter fault. The induction motor has a rotor cage structure that includes metal (copper or aluminum) for the conducting bar and an end-ring, and the thermal and mechanical analyses are different and more important than in the permanent magnet motor. In this paper, a 60kW-12,000rpm induction motor with a copper die-casted rotor was developed for a traction motor considering mechanical and thermal problems. The electromagnetic dimensions of motor were determined from an induction motor equivalent circuit and verified from FEM analysis in various operating conditions. The design results for the EV traction motor were also verified through experimental tests based on continuous (30kW) and maximum (60kW) operating conditions.

## References

- [1] Gianmario Pellegrino, Alfredo Vagati, Barbara Boazzo, and Paolo Guglielmi, "Comparison of Induction and PM Synchronous Motor Drives for EV Application Including Design Examples" *IEEE Transactions on Industry Applications*, Vol. 48, No. 6, pp. 2322-2332, 2012.
- [2] Z. Rahman, M. Ehsani, and K. Butler, "An investigation of electric motor drive characteristics for EV and HEV propulsion systems," in *Proc. SAE Future Transportation Technology Conf.*, Costa Mesa, CA, Aug. 2000, Paper No. 2000-01-3062.
- [3] Yildirim, M., Polat, M., and Kurum, H., "A survey on comparison of electric motor types and drives used for electric vehicles," *Power Electronics and Motion Control Conference and Exposition (PEMC)*, pp. 218-223, 2014.
- [4] Hashemnia, N. and Asaei, B., "Comparative study of using different electric motors in the electric vehicles," *Proceedings of ICEM 2008*, pp. 1-5, 2008.
- [5] A. Arkkio, "Finite element analysis of cage induction motors fed by static frequency converters", *IEEE Transactions on Magnetics*, Vol. 26, No. 2, pp 551-554, 1990.
- [6] L. Alberti, N. Bianchi, and S. Bolognani, "Variable-speed induction machine performance computed using finite-element," *IEEE Transactions on Industry Applications*, Vol. 47, No. 2, pp. 789-797, 2011.
- [7] P. W. Han, D.J. Kim, Y.D. Chun, J.H. Choi, U.J. Seo, and D. H. Koo, "The study on the design parameters and losses of copper die-casting induction motor for high speed," *International Journal of Applied Electromagnetics and Mechanics*, Vol. 41, Number 1-4, pp. 949-955, 2014.
- [8] B. C. Woo, D. K Hong, D. H. Koo, Y. D Chun, J. H. Choi and P. W. Han, "Development of 10kW Multi-gate-based Copper Die-casting High Speed 3 Phase Induction Motor," *Proceedings of KIEE Summer Conference*, pp. 1133-1134, 2011.



**Yon-Do Chun** He received the B.S., M.S. and Ph.D. degrees in Electrical Engineering from Hanyang University in 1996, 1998 and 2001, respectively. From 2001 to 2003, he received a fellowship from the Japan Society for the Promotion of Science (JSPS), and he was with the Department of Electrical Engineering at Waseda University as a visiting scholar. From 2004 to 2012, he worked at the Korea Electrotechnology Research Institute (KERI). He is currently a chief researcher, Principal Researcher and technical leader of the Electric Motor Research Center, KERI.



**Byoung-Gun Park** He received his B.S. in Electrical Engineering from Myongji University, Yongin, Korea, in 2005, and his M.S. and Ph.D. in Electrical Engineering from Hanyang University, Seoul, Korea, in 2007 and 2011, respectively. Since 2011, he has been with the Korea Electrotechnology Research Institute (KERI), Changwon, Korea, where he is currently a Senior Researcher in the Electric Motor Research Center.



**Dong-Jun Kim** He received the B.S degree in Electrical Engineering in 2004 from Kyungnam University. He received the M.S degree in Electrical Engineering in 2013 from Changwon National University. He has worked at the Korea Electrotechnology Research Institute (KERI). He is currently a senior Engineer of the Electric Motor Research Center, KERI.



**Jae-Hak Choi** He received the B.S., M.S., and Ph.D. degrees in Electrical Engineering from Hanyang University in 1999, 2001 and 2005, respectively. From 2005 to 2007, he worked at LG electronics. Since 2008, he has worked at the Korea Electrotechnology Research Institute (KERI). He is currently a senior researcher of the Electric Motor Research Center, KERI.



**Pil-Wan Han** He received the B.S., M.S. and Ph.D. degrees in Electrical Engineering from Hanyang University in 1998, 2000 and 2013, respectively. From 2000 to 2005, he worked at LG electronics. Since 2005, he has worked at the Korea Electrotechnology Research Institute (KERI). He is currently a senior researcher of the Electric Motor Research Center, KERI.



**Suk-kee Um** He received his Ph.D. degree in Mechanical Engineering from Pennsylvania State University in 2003. Currently he is working for Hanyang University as an associate professor in the School of Mechanical Engineering, Hanyang University, Seoul, Korea since 2007. His expertise includes heat and mass transfer in advanced green energy systems.